Mechatronics 36 (2016) 136–146

Contents lists available at ScienceDirect

Mechatronics

journal homepage: www.elsevier.com/locate/mechatronics

The hybrid OmniClimber robot: Wheel based climbing, arm based plane transition, and switchable magnet adhesion

Mahmoud Tavakoli[a,*], João Lourenço[a], Carlos Viegas[a], Pedro Neto[b], Anibal T. de Almeida[a]

[a] Institute of Systems and Robotics, University of Coimbra, Portugal
[b] Department of Mechanical Engineering, University of Coimbra, Portugal

ARTICLE INFO

Article history:
Received 3 September 2015
Revised 11 March 2016
Accepted 23 March 2016
Available online 14 April 2016

Keywords:
Climbing Robots
Omnidirectional Wheel
Switchable Magnets
Hybrid climbing mechanism

ABSTRACT

Climbing robots that integrate an articulated arm as their main climbing mechanism can eventually take advantage of their arm for plane transition and thus to operate on 3D structures rather than only climbing planar surfaces. However, they are usually slower than wheel based climbing robots. Within this research we address this problem by integration of a light-weight arm and adhesion mechanism into an omnidirectional wheel based climbing robot, thus forming a hybrid mechanism that is agile in climbing and still able to perform plane transition. A 2DOF (Degree of Freedom) plannar mechanism with 2 linear actuators was designed as a light-weight manipulator for the transition mechanism. Furthermore, we customized and developed actuated switchable magnets both for the robot chassis and also as the adhesion unit of the arm. These units allow us to control the amount of magnetic adhesion force, resulting in better adaptation to different surface characteristics. The adhesion units are safe for climbing applications with a very small power consumption. The conceptual and the detailed design of the mechanisms are presented. The robots were developed and successfully tested on a ferromagnetic structure.

1. Introduction

Climbing robots have been developed and widely used in industry in the last couple of decades, to respond to the need of a tool capable of performing specific work of inspection and maintenance on tall structures. Besides inspection they perform repairs, painting, cleaning and other maintenance tasks in hard to reach or hazardous locations.

Most of the climbing robots which have been developed so far can be roughly categorized to the following group:

- Multi degrees of freedom (DOF) serial, parallel or hybrid arms (step by step based climbing robots);
- Multi-legged climbing robots;
- Wheel based climbing robots.

Climbing robots developed in the first category are usually miniature sized robots and are not indicated for industrial purposes [1–3]. Some of them rely also on relatively soft and penetrable surface materials such as cloth, wood or cork. Multi DOF arms usually offer good maneuvering over 3D structures. The arm can be serial [4–6], parallel [7] or hybrid [8]. However, these robots are generally heavy, big and complex. To be able to pass bends, these robots employ at least 4 DOF [6,8,9] and usually have a mass of more than 20 kg. Due to such problems, these robots could not find their way out of the laboratories. Wheel based climbing robots are generally faster than the other two groups, but they have less maneuverability compared to multi leg climbing robots. Most wheeled climbing robots are only capable of navigating on simple structures without obstacles, bends or branches [10–12]. Two of the most important abilities that makes a climbing robot more appropriate for industrial applications are the ability to overcome obstacles in its path, and the ability to transit between perpendicular planes. This is important since most of the complex industrial installations, such as the one shown in Fig. 1, include surfaces with some sort of obstacles, such as ridges, flanges and gaps. When these obstacles are unsurpassable, the robot should be able to find a way to go around, which most of the time involves plane transitions.

Even if none of the above obstacles are present on the structure, just the ability of the robot to move on the ground and then transit to a vertical surface and vice versa increases its autonomy. Some wheel based climbing robots have used innovative features to solve some of these problems. Strategies adopted include:

- Use of relative scale, by employing very small robots when compared with the size of the obstacle, so the robot can

* Corresponding author. Tel.: +351968397681.
E-mail address: mahmoud@isr.uc.pt, mahmood.tavakoli@gmail.com (M. Tavakoli).

http://dx.doi.org/10.1016/j.mechatronics.2016.03.007
0957-4158/

Fig. 1. Environment for service climbing robots. Sines refinery in Portugal.

navigate on the obstacle like it normally navigates on the surface [13]. This is for instance true in the Magnebike: a compact magnetic wheeled inspection robot [14]. This robot benefits from small magnetic wheels and is designed to work on narrow surfaces and tight spaces. It uses a wheel lifting mechanism for overcoming obstacles and performing plane transitions.

- Using linear effectors and legs to overcome the obstacle [15], relying on obstacles and surface features of a specific size.
- Using complex hybrid locomotion mechanisms which combine the principles of wheels and legs (walking wheels concept) [16].
- Using multi-robot collaboration to connect multiple units and transpose obstacles together [17]. The Alicia3 is a single robot composed of three separate modules which are connected through links [18]. Each module has an adhesion device based on suction and wheels for locomotion. The advantage of this articulated design is that it allows to overcome small obstacles such as gaps or ridges on the walls, by detaching one of the modules at a time and moving it over the obstacle. Even plane transition is not reported with Alicia3, but this concept should also allow the robot to perform plane transitions. However, this results in very high torque demands on the joints due to the relatively heavy climbing modules (4 kg each module) and the long arms.

However, most service robots are too large to use their relative scale as an advantage to help them overcoming the obstacles in their environment. Use of multi-legged robots or hybrid locomotion for climbing purposes requires greater number of DOFs, without necessarily improving the ability of robots to progress in a complex workspace. Using multi-robot collaboration suggests a complex operation and control scenario which is not desirable for industrial applications that demand for simple and reliable solutions.

Recently, a plane transition mechanism based on a 2DOF arm was proposed for the OmniClimber, magnetic wheeled climbing robot [19]. Although it successfully managed to perform plane transitions, the conventional serial arms may not be an optimal solution for this problem, due to the high torque demands on the joints to support the weight of the robot during plane transition. This results in need for relatively heavy actuators which increases the overall size and weight of the robot. Even though with an innovative design of the arm mechanism we could use one actuator rather than two for the 2DOF arm, it was still not optimal since the complicated transmission mechanism made the system bulky and not very light weight (662 g arm with the adhesion unit assembly). The other problem was that the adhesion unit of single DOF arm was based on electromagnets, which require constant power supply to maintain the attachment force. This results in a decreased power autonomy and also it presents safety concerns in case of power failure.

To address these limitations, in this research work we present a new version of OmniClimber with a novel 2DOF transition mechanism. Also the electromagnetic adhesion unit was replaced by actuated switchable magnets (SM). A similar switchable magnet unit was developed as the main adhesion unit of the robot's chassis which enables the robot to control its adhesion force.

In spite of being used for many years in industrial applications, switchable magnets received less attention in the scientific community. However, recently some research works focused on application of SMs in mobile robots. *Miche* robots [20], use switchable magnets driven by a servo motor on their sides for self-assembly of individual actuated modules. Switchable magnets have also been used in mobile robots such as *TERMO* an inspection step by step based robot for ferromagnetic structures [21] and in *Tubulo* a train-like inspection robot for ferromagnetic tubes.

Rochat et. al. discussed development of different types of switchable magnets for applications in mobile robots [22]. Switchable magnets, present the advantages of not requiring a constant power supply to maintain their state, but instead only when switching states. They also offer the possibility to vary the magnetic force from almost zero to maximum, thus enabling real time dynamic adjustment of the adhesion properties of the robot.

In this article, we first present the design and development of a light-weight actuated switchable magnet unit, to be used as the adhesion unit on OmniClimbers. Second, by application of a non back-drivable actuation system, we enable force control by the switchable magnet unit, with minimum power consumption. This unit was integrated not only on the transition arm, but also on the chassis of the robot. Third, we present the design, kinematics, development and integration of a light weight 2DOF planar manipulator. Fourth, we present design and integration of an ad-hoc control board for the omniclimbers and finally we demonstrate the plane transisiton with the novel Omniclimber robot.

2. OmniClimber

The OmniClimber, is an omnidirectional climbing robot for inspection of ferromagnetic structures [23]. It is capable of navigating on both flat and curved surfaces with good maneuverability, thanks to its passive curvature adaptation mechanism, its magnetic adhesion mechanisms and through the use of three custom made magnetic omnidirectional wheels [24,25]. Taking advantage of its magnetic omni directional wheels, the holonomic drive robot can move in any direction on vertical surfaces without requiring to change its yaw angle. In addition we addressed the motion control of an omnidirectional climbing robot based on dead reckoning method [26]. In order to be able to transit between planes and overcome obstacles, we decided to integrate an articulated arm with a magnetic adhesion unit as its end effector. Through this hybrid system, we combined the advantages of a wheel based climbing robot (speed and simplicity), with advantages of the articulated climbing robots (maneuverability in 3D structures).

The characteristics of the last version of the OmniClimber are stated in Table 1.

The transition mechanism from the previous version, shown in Fig. 2, had several novelties like the use of only one actuator to control two joints at different speeds and time intervals.

The first joint, which connects both motor and arm link, rotates 90 degrees to perform the whole plane passing. Meanwhile, and with a time gap to avoid collisions between the robot and the planar surfaces, the second joint, which connects the arm link to the robot, rotates full 180 degrees, thanks to the geared transmission to the first joint, as shown in Fig. 3.

However, and despite using only one actuator, the transmission and hardware needed for such a complex design made the whole arm too heavy for a small climbing robot such as the OmniClimber.

Table 1
OmniClimber characteristics.

Diameter × height Mass	197 × 84 mm 1110 g
Actuation	3 Dynamixel MX-64 rotary actuators
Mechatronics and control	Stand-alone robotic system with integrated control board on the chassis and IR module
Power	Onboard LiPo 1000 mAh battery
Wheels	3 Omnidirectional Magnetic Wheels 70 mm diam.
Min adhesion force[a]	25,5 N (chassis electro-magnet *off*) 45,0 N (chassis electro-magnet *on*)
Max climbing speed	14 cm/s
90º plane transition time	5 s
Max payload[a]	1200 g
Movement	Full omnidirectional

[a] Measured on a 1 mm thick sheet of steel.

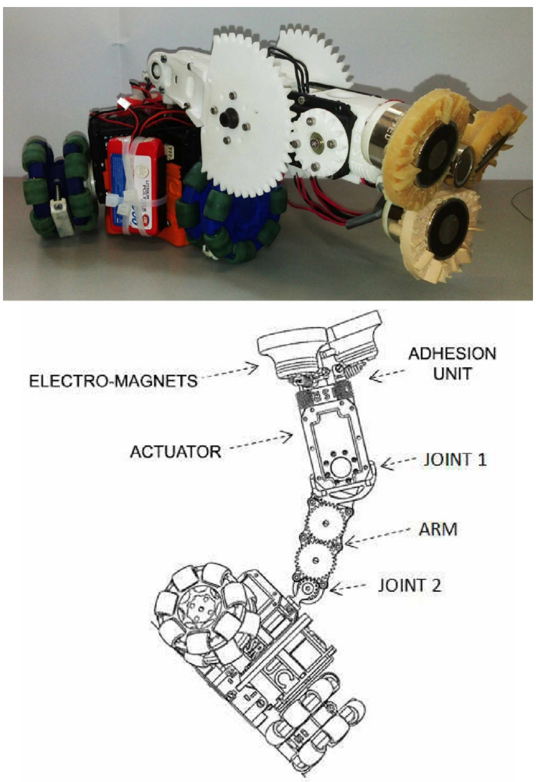

Fig. 2. Previous version of Omniclimber transition mechanism [19].

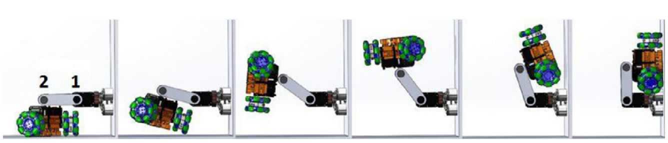

Fig. 3. Plane transition routine frames.

Also, since it relied on electromagnets, it needed an extra battery to power them, thus increasing even more the total weight of this solution. So in the new version of the OmniClimber we proposed a novel transition mechanism with integrated switchable magnets which is lighter and has adhesion force control capabilities.

3. Switchable magnets for climbing robot applications

A switchable magnet is a system which uses moving permanent magnets to change the magnetic flux path to the inside or outside of the device, thus enabling to virtually turn *on* or *off* the magnetic attraction force of the whole system. We used a commercially available switchable magnet, MagJig 95, shown in Fig. 4, as a start point for the development of a more optimized SM for climbing robot applications. MagJig 95 consists of one circular 20 mm fixed permanent magnet below another circular 20 mm moving magnet. Both magnets are inside an iron housing. The device possesses an handle coupled to its top to allow the user to manually rotate the moving magnet. Total height of the magnets housing is 22 mm, while its section is 28 mm by 21 mm.

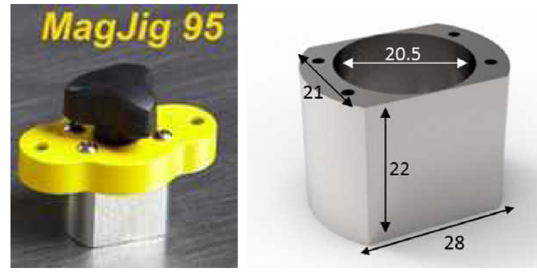

Fig. 4. Magjig 95, with the magnets housing dimensions.

Table 2
Simulation results shows the magnetic flux path on section view and the holding force. Left: MagJig 95, Right: Similar device with plastic housing.

Device *on*	Device *off*	Device *on*	Device *off*
338.4 N	1.4 N	59.3 N	26.8 N

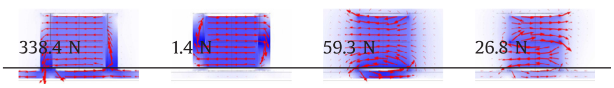

The goal was to modify this design to reach a better holding force per unit of mass and a better geometry for the climbing robots applications. For the adhesion unit of a climbing robot, a low profile (low height) mechanism is preferred since it results in a smaller detachment torque.

For the design of the new adhesion unit, we started by simulating the commercially available MagJig 95 magnets in *Comsol Multiphysics 4.3* [27], a finite element analysis solver package for various physics and engineering applications, to observe the magnetic flux in the magnets, the housing and the object in both states of *on* and *off* and estimate the magnetic attraction force. We then tested the real unit and compared the results obtained with the ones from the simulations, to validate our simulation parameters. Then, we analyzed the effect of the housing material; the Housing shape, and the housing and magnets diameter in the overall performance of each solution.

As a start point we simulated the commercial SM in both states of *on* and *off* against a ferromagnetic metal surface with a thickness of 3 mm and compared it with a similar device with a plastic housing. As we see in Table 2 the flux between opposite poles goes though the surface when the device is *on*, and through the housing when it is *off*, as expected. In practical experiments the maximum force achieved was of 324.8 N, close to the value achieved in the simulations (338.4 N). However the plastic housing has a holding force of 59.3 N, and thus was discarded as an option. This can be explained by the lack of a conductive core to direct and concentrate the magnetic flux, clearly visible on the representations of the flux path.

The original housing of the *MagJig* 95 unit, includes two flat cuts at two sides. To understand the role of these flat cuts we made simulations with a steel fully circular housing, without the flat cuts. As can be seen in Table 3, the holding force is much smaller when the device is on (81.6 N vs 338.4 N), since in this case a significant amount of magnetic flux passes through the housing, and not through the object that should be grasped. A fully cylindrical housing provides a path for the flux to go around the

Table 3
Simulation of a circular magnet housing, showing the magnetic flux path on both top and section view, and the holding force calculated below.

Device *on*	Device *off*
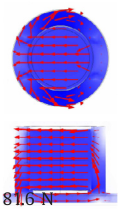	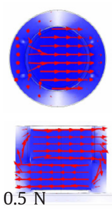
81.6 N	0.5 N

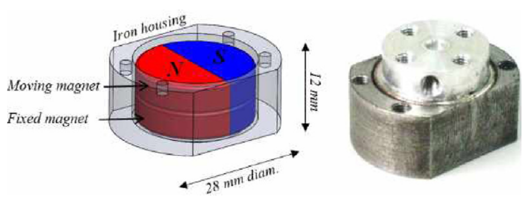

Fig. 5. Novel switchable magnet developed for climbing robot applications.

Table 4
Comparison between the *MagJig* 95 and the novel device.

	MagJig 95	Novel device	Variation
Mass [g]	87.7	42.1	–52%
1 mm steel:			
Holding force [N]	112.6	100.1	–11%
Force/Mass ratio [N/g]	1.28	2.38	+85%
3 mm steel:			
Holding force [N]	338.4	183.4	–46%
Force/Mass ratio [N/g]	3.86	4.36	+13%
Detaching torque [N.m]	0.094	0.025	–73%

housing axis, from one magnetic pole to the other, thus not forcing the flux to pass through the bottom surface resulting in a significant reduction of the adhesion force.

In order to study the effect of the diameter of the chamber and the magnet, we achieved a series of simulation to reach to the highest Force/Mass ratio which resulted in a chamber of (Ø28 × 12 mm) made from AISI 1018, with a permanent magnet of (Ø20) mm as the best trade-off. The new switchable magnet developed for climbing robot applications is depicted in Fig. 5.

3.1. Comparison

We tested the device on a 1 mm thick steel plate and also on a 3 mm thick steel plate, then comparing the adhesion force of the new unit with the one from *MagJig* 95.

As can be seen in Table 4, for both cases of 1 mm steel and 3 mm steel, the adhesion force/mass ratio is improved comparing to the *MagJig* 95. In case of the 1 mm steel, this ratio was increased 85%, while for the 3 mm steel, the increase was 13%. This is mainly due to the fact that in thin plates, most of the large magnetic field of the *MagJig* 95 is not used, while the magnetic field on the novel device is much more focused on the region closer to the surface of the plate, thus is used more efficiently. This effect is depicted in Fig. 6. Furthermore, there is a significant reduction of the detaching torque of 73%.

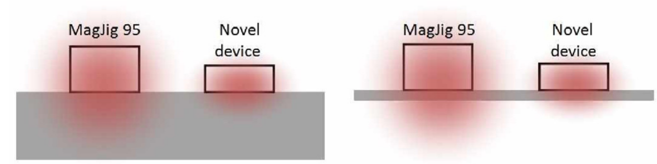

Fig. 6. Comparison between the magnetic field of the MagJig 95 and of the novel device in plates with different thickness.

4. A central magnet with adjustable adhesion force

The ability to control and adjust the magnetic force generated by the OmniClimber's central magnet is extremely important in the following scenarios:

- When the robot is passing from one plane to the other and to facilitate detachment of the robot from the surface, one should be able to switch off the magnetic adhesion force. When the robot is extending the arm for performing an inspection task, or to make a plane transition, additional detaching forces are applied to the chassis of the robot. In this case an increase in the adhesion force of the chassis is necessary.
- When the robot is moving upside down the magnetic adhesion force should be superior to when it is moving vertically or on top of the surface.
- When the robot moves to another structure and the surface material or thickness changes, the magnetic force generated should be adjusted to the new conditions.

One of the problems of the previous version of the OmniClimber was that in order to adjust the magnetic force, one had to manually adjust the position of the central magnet unit inside the robot chassis. This was not optimal and presented a severe limitation in all of the scenarios mentioned.

Therefore we set out to integrate a remotely controllable force adjustment mechanism, to not only turn the magnets *on* and *off*, but also to control the adhesion force. One possible method was to integrate an actuator to move the central magnet inside the chassis. To do this one has to use a rotary to linear transformation mechanism. By controlling the distance between the central permanent magnet and the surface, one could control the magnetic adhesion force. This effect can be roughly translated by the following empirical expression given by magnets manufacture HKCM [28]:

$$F_r = \frac{F_h}{1+s} \quad (1)$$

Were F_h is the Magnetic force depending on the material and s the distance between the magnet and the surface.

One could use an electromagnet but then it would have its limitations, such as safety problems in the event of power failure.

The solution adopted was to use an actuated switchable magnet. This results in a simpler, more compact and fail-safe mechanism. This solution also has the advantage of:

- Being able to control the force, and not only to switch the magnet *on* and *off*.
- Being a non back drivable mechanism, meaning that it consumes energy to rotate one of the permanent magnets, but after reaching the desired angle position the actuators can be turned off while remaining in that same position and not consuming any energy.

Adhesion force changes based on the angle of the upper magnet relative to the lower magnet, as magnetic fields align and reorient. We set out to measure in detail this variation by first running a simulation in COMSOL of the magnetic flux and the adhesion force

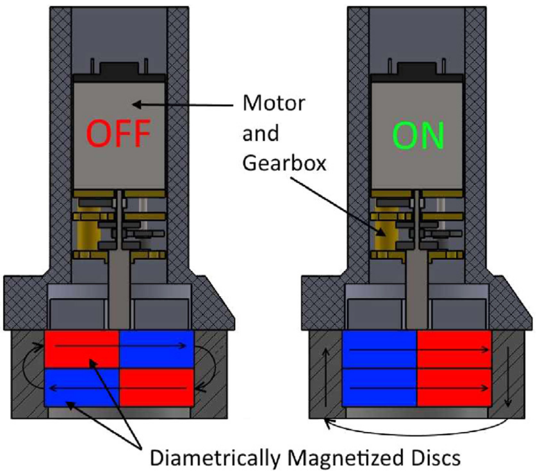

Fig. 7. Magnetic flux in *on* and *off* states.

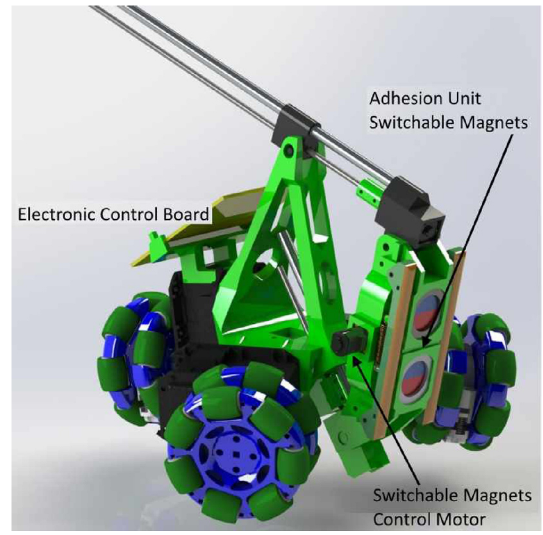

Fig. 8. Current version of OmniClimber with the transition mechanism closed.

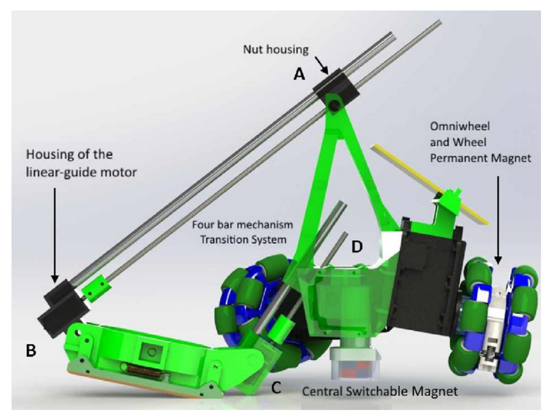

Fig. 9. Current version of OmniClimber with the transition mechanism open and central magnet in detail.

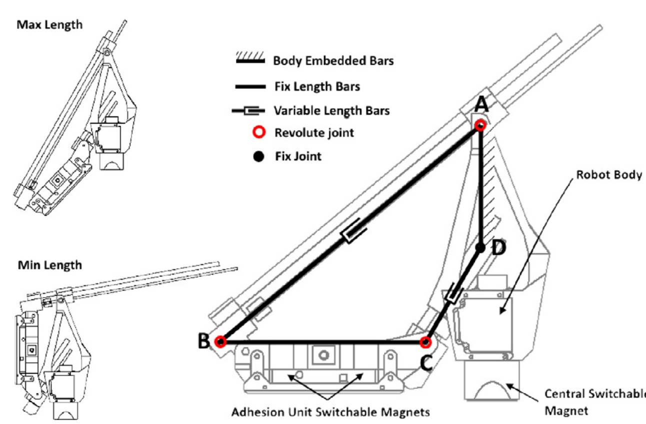

Fig. 10. Transition mechanism.

obtained for different angles and then by measuring the adhesion force experimentally in a prototype.

The force generated by a switchable magnet varies with the orientation of the poles of the magnets inside. The magnetic flux always occurs between opposite poles. Thus if the poles of both magnets are aligned the magnetic flow is forced down the casing through the surface material to re-enter the housing on the opposite side. When this happens, the switchable magnet generates an attractive force proportional to the alignment of magnets. If the poles are fully aligned the generated force is maximum. If they are not aligned, strength decreases because part of the flux circulates between the two magnets instead of going down to the surface. If the poles are completely inverted, the magnetic flux flows directly between the magnets and the switchable magnet does not generate any force of attraction, as shown in Fig. 7. Due to small leaks in the housing thin side there is always a residual attraction force.

Though it is possible to select and maintain a state between *on* and *off* on the switchable magnet, the magnetic forces between the two magnets force them to move to one of the those two preferential positions. So to maintain the top magnet at a desired angle, so that the mechanism is non back drivable, it is necessary to counter the torque which tries to align the upper magnet with the lower one. For this, we selected an actuator whose internal friction is big enough to stop the shaft's rotation due to the torque exerted by the two magnets. In this case we used a Pololu Micro HP with 298:1 transmission ratio.

5. Novel plane transition mechanism using switchable magnets

The new transition mechanism shown in Figs. 9 and 10 is a 2 DOF planar manipulator that embeds two linear actuators. The length of two links of the mechanism are controlled by two lead screw systems. Such mechanism is able to provide 2 degrees of freedom between the robot chassis and the end effector as can be seen in Fig. 8. By changing the length of the two variable length bars, it is possible to change the distance and angle between the adhesion unit (manipulator) and the chassis which is necessary for the plane transition. Both end effector, and chassis are equipped with a switchable magnet system. Depnding on the direction of the transition, the role of chassis and end effector change. That is, one of them acts as a fixed base, and the other acts as the manipulator.

Linear movements are created by a nut and screw system with linear guides. This solution results in a very high transformation ratio which allows the use of very small and light-weight actuators (Pololu Micro HP 100:1 gear motor, weight = 9.5 g) at a cost of the speed reduction (0.5 mm per rotation with the motor running at approximately 300 rpm). Here the speed is less significant because plane transition does not happen very often.

5.1. Adhesion unit

The adhesion unit of the arm should be able to support the full weight of the robot and also the detaching torque during the plane transition. This adhesion unit possesses two switchable magnets at a certain distance from each other.

As can be seen in Fig. 12, d is the distance between the center of the adhesion unit and the anchor point and s is the distance between the center of switchable magnets. These distances are calculated so that the force generated by the switchable magnets of the arm adhesion unit is sufficient to support the torque generated by the weight of the robot. The other distance in the diagram of the Fig. 12 is (D), which is the distance between the robot body's center of mass to the anchor point. The torque generated by the weight of the robot T_W is function of this distance and is given by:

$$T_W = D \times F_w \quad (2)$$

The maximum torque is generated for the highest value of distance (D) which is 120 mm. The torque in this situation is:

$$T_W = 0.120 \times (1.120 \times 9.81) = 1.32 \text{ Nm} \quad (3)$$

Where T_W is the torque generated by the weight F_W.

To support the robot weight the distance (d) must be such that the value of torque generated by the switchable magnets T_{AU} is greater than that generated by the weight of the robot:

$$T_{AU} \geq T_W \quad (4)$$

For this to happen (d) is given by:

$$d = \frac{T_{AU}}{F_{SM}} \quad (5)$$

Where $T_{AU} = T_W$ and F_{SM} is the force generated by the two switchable magnets. Therefore (d) is:

$$d = \frac{1.32\,\text{Nm}}{116\,\text{N}} = 11.4\,\text{mm} \quad (6)$$

The distance (d) that we chose was 20 mm for a safety factor of 1.7.

The distance (s) can be obtained by dividing the generated torque of the weight by the force of each switchable magnet:

$$s = \frac{1.32\,\text{Nm}}{58\,\text{N}} \geq 0.023 \text{ m} \quad (7)$$

Here we chose s = 34 mm in order to respect the SM dimensions which results in a safety factor of 1.5.

Both switchable magnets can be actuated by a single motor, through a non back-drivable worm gear mechanism. The required torque to actuate the two switchable magnets varies with proximity to a ferromagnetic surfaces. The worst case scenario happens in the absence of any ferromagnetic surface or material. In this case each SM unit requires 0.25 Nm to turn, or 0.5 Nm in total.

Here we used a MICRO HP Pololu gear motor with a gear ratio of 100:1 which is coupled with an additional custom made worm drive transmission increasing its gear ratio 28 times providing more than 1 Nm at the output shaft considering a 50% efficiency on the worm drive transmission.

Furthermore, we integrated a mechanism, called "Skis", which is used to increase the friction between the robot and the surface, thus reducing the risk of slippage when the robot is stationary and held only by the adhesion unit on a vertical surface (Fig. 11). In the beginning of the transition the robot is in contact with the surface with only two wheels. During our experiments we saw that at this point while the robot returns to its normal position with the three wheels in contact some slippage happens on the adhesion unit. To prevent this from happening it is necessary to create friction. The problem is that the friction hinders the movement of the robot. So the developed solution has to prevent slipping without hampering the progression of the robot on the surface. To do this the bottom side of the Skis is covered with an high friction silicon rubber.

As shown in Fig. 13 when the robot is stationary the weight of the robot pushes the skies against the surface preventing it from happening. In the opposite situation, when the robot is climbing, the Skis retreat.

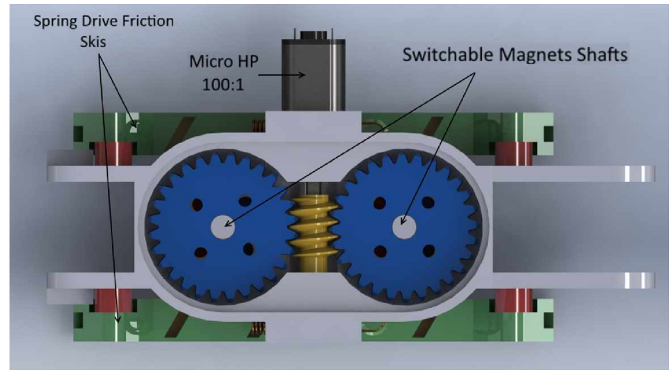

Fig. 11. Adhesion unit worm drive transmission and friction skis.

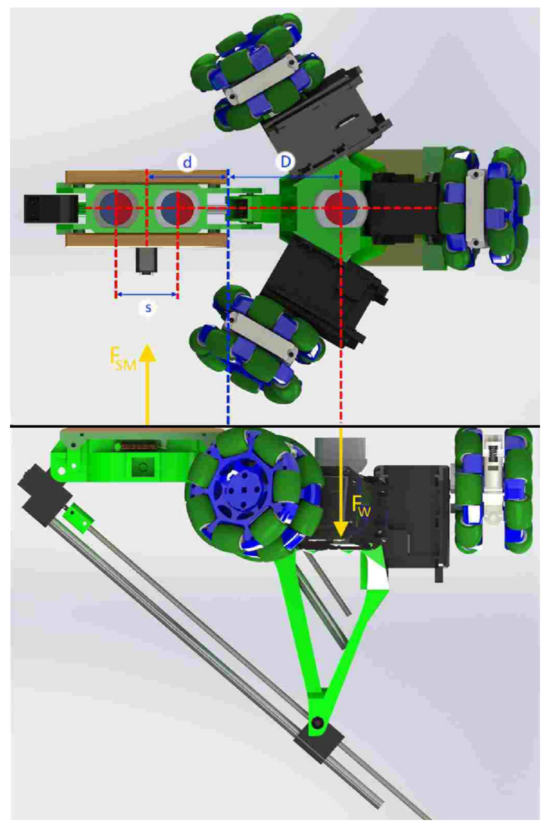

Fig. 12. Distances and forces diagram.

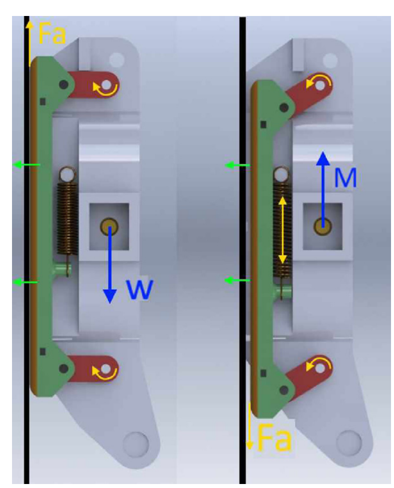

Fig. 13. Anti slip system (Fa - friction force; W - weight; M - movement force).

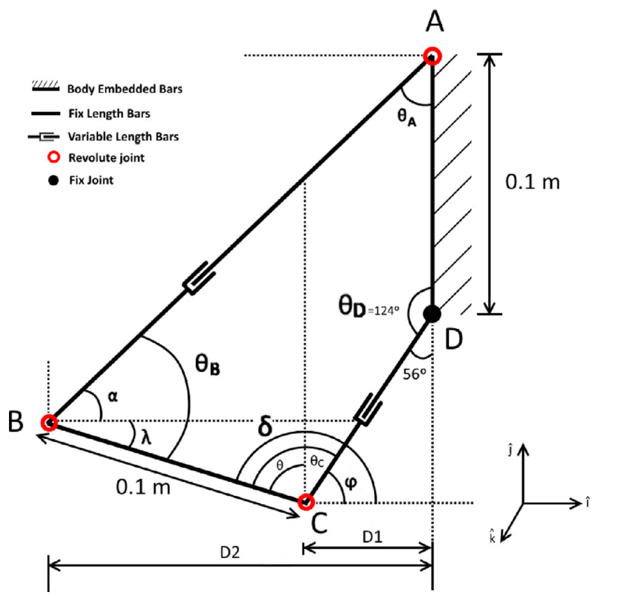

Fig. 14. Transition mechanism simplification.

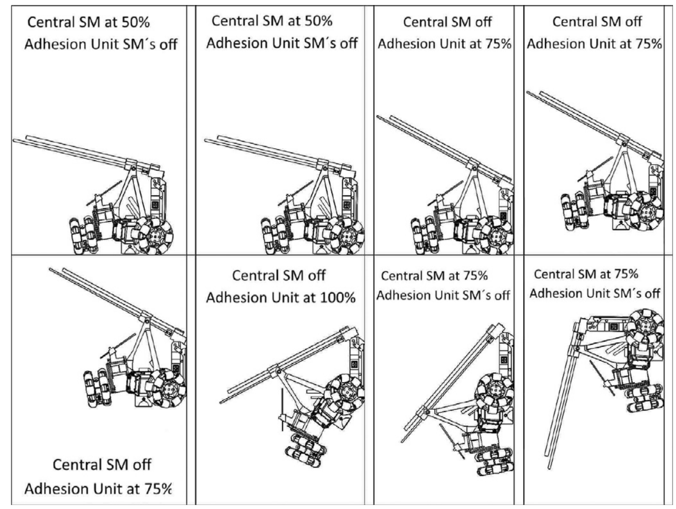

Fig. 15. Plane transition process with the new mechanism.

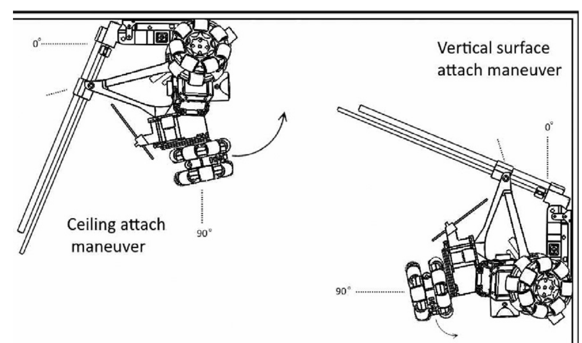

Fig. 16. Ceilling and vertical wall maneuvers.

5.2. Kinematics and control

Fig. 10 , depict the chain of the 2DOF planar mechanism. Points A and D have fixed positions and the angle between AD and CD is also fixed. The bar CD does not rotate but its length varies. Bar AB has both length variation and rotation on both vertices's. BC has also a fixed length. The inverse kinematics of the mechanisms allows us to calculate the length of the two variant length bars ((AB) and (CD)) linear guides, based on the desired pose between the two adhesion units i.e. the relative inclination between the adhesion units (90+θ) and its distance (D1), as shown in the Fig. 14. The following expressions provide the lengths of the variant length bars, i.e., $l_1 = |AB|$ and $l_2 = |CD|$ based on the required inputs (d = D1 and θ)

$$l_2 = \left(\frac{D1}{\cos\varphi}\right) \tag{8}$$

$$l_1 = \sqrt{(D2)^2 + ((AD + CD \times \sin\varphi) - BC \times \cos\theta)^2} \tag{9}$$

Where:

$$D2 = D1 + (BC \times \sin\theta) \tag{10}$$

and φ is a constant angle: $\varphi = 180^\circ - 56^\circ = 124^\circ$.

5.3. Transition

Fig. 15 depicts the transition process. To make the transition first the adhesion unit of the arm is placed in parallel to the new surface. Once the contact is established the SM unit of the chassis is turned off. In this case only two of the three wheels are in touch with the surface. These two wheels lift the robot. In this case the adhesion force is provided by the SM unit of the arm. But the adhesion force is adjusted to a minimum necessary adhesion force that is required to support the robot's weight and provide enough traction to the wheels for climbing. This is determined experimentally and depends on the material and the thickness of the structure. For instance for the case of this experiment which was performed on a 1mm thin steel plate, this value was around 75% of the maximum adhesion force. The robot climbs with two wheels to an extent in which it is possible to attach the third wheel. The attachment of the third wheel is performed with the help of the arm (as shown in Fig. 15). In this case the SM unit of the arm provides the maximum adhesion force and acts as a safe anchor to overcome the generated torques by the weight of the robot. Afterwards the SM unit of the arm is turned off and the arm return to its original pose before the transition.

5.4. Torque analysis and actuator selection

The forces and torques involved during the transition between planes depend on their orientation relative to gravity acceleration vector. This means that the loads which the mechanism will have to support will be different when the transition is made between the ceiling and the vertical wall or between the ground and the vertical wall, as shown in Fig. 16. These cases were studied and the actuators used in the transition mechanism were dimensioned taking into account the requirements for the most demanding transition.

The mechanism should provide the required torque to rotate the joint in the worst case scenario, which is the passage from a vertical wall to the ceiling. As can be seen in Fig. 17, we have:

Weight [N];

$$F_w = W \times \cos(\alpha)$$

Torque [Nm];

$$T = d \times (W \times \cos(\alpha))$$

Here α is variable during the transition and "*d*" represents the distance between the center of the mass of the robot and the joint C on the arm adhesion unit.

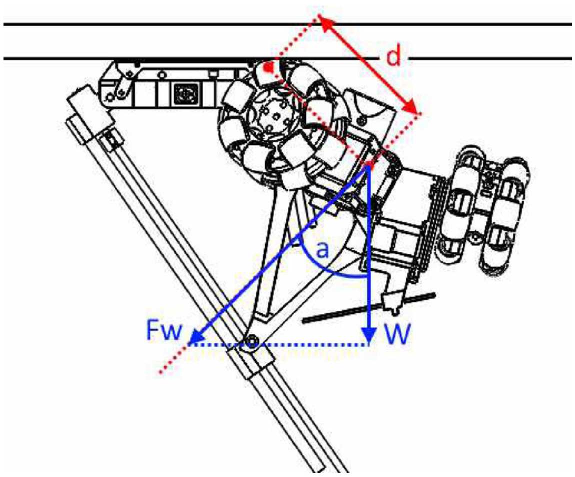

Fig. 17. Gravity force and weight vectors during the ceiling attach maneuver.

Based on these results the actuators for the linear guides are selected. Due to the large contact area between the threads of the nut and the threads of the shaft, there is a huge loss of energy in friction so we considered just a 20% efficiency for the screw-nut system. The force generated by threaded shafts can be calculated as:

$$F_{out} = \left(\frac{2\pi \times T_{in}}{p} \times \eta\right) \tag{11}$$

Where F_{out} determines the generated linear force and T_{in} is the torque of the chosen motor. F_{out} is also the force that the shafts applied in the joints A and D. This force must be sufficient to counteract the weight of the robot and force this to return its position after the transition. In the worst scenario the force F_{out} applied in joint A must generate at least 1.32 Nm, as depicted in Fig 22. p is the pitch which is 0.5 mm for an M3 screw, and η is the efficiency. The selected actuators are Pololu Micros Hp with a gear ratio of 100:1 and a nominal torque of 0.21 Nm at output shaft. This corresponds to a force of 0.53 N, assuming an efficiency of 20%.

This actuator is quite small. It has a cross section of 10 × 12 mm with a length of 26 mm and weights approximately 10 g. The high transmission ratio not only allows the use of smaller actuators, it also makes the system not non back drivable, having as a consequence the increase in transition time. Nevertheless, this does not seem to be critical since the plane transition is not a very frequent action.

6. Mechatronics

The new version of the Omniclimber integrates seven actuators from two different series (compared to four actuators in the previous version of the hand from a single servo, i.e., dynamixel actuators). Therefore, the control of the robot is more complicated. In order to avoid integration of several drivers and control boards, we opted to design an ad-hoc single board control unit for processing, for driving all actuators of the robot and the arm, and also for communication. Fig. 18 shows the schematic of the control unit and also the home-made board.

The integrated micro-controller is an ARM Cortex STM32F4. The Dynamixel servos of the climbing robot use a TTL protocol. To communicate with the micro-controller's the TTL must be converted from half-duplex to full-duplex. This is accomplished using a Buffer (SN74LS241DW) to switch between UART's TX and RX. The servos are connected in a Daisy Chain configuration which means that all servos receive all communication messages and select which message is for him by searching for a message with an ID that matches its own.

The Gear motors of the arm and the switchable magnets are driven with PWM using a H-Bridge (DRV8801PWP). They are

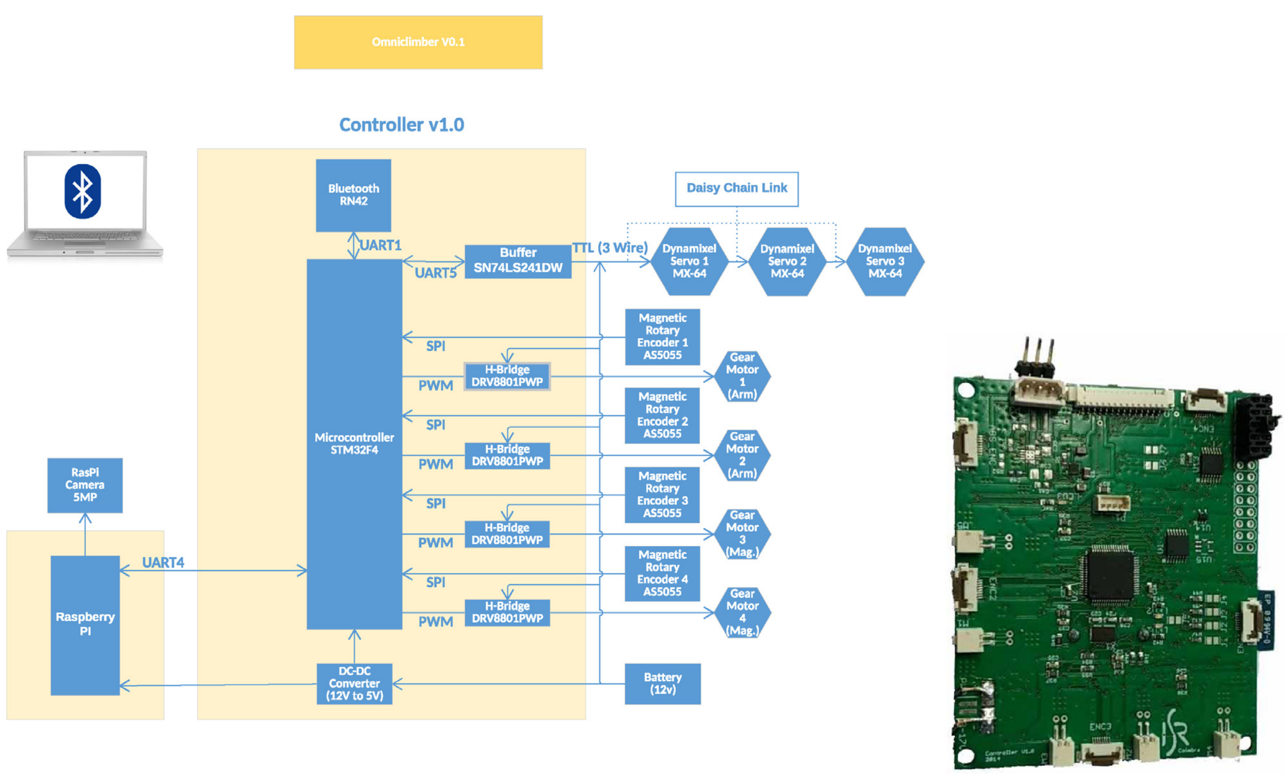

Fig. 18. The schematics of the processing and control unit.

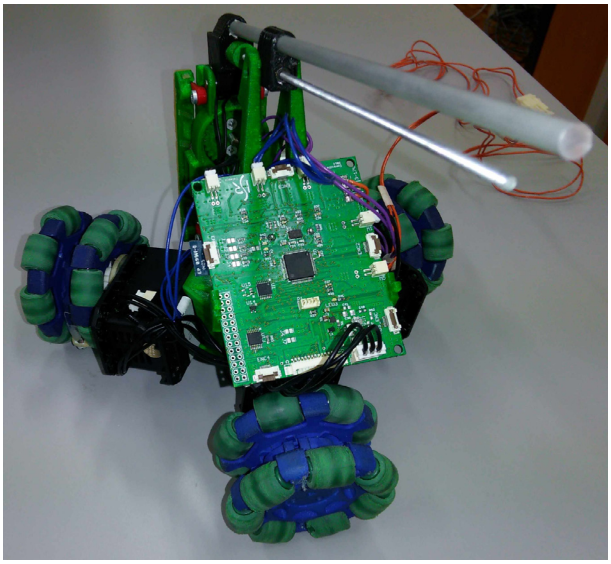

Fig. 19. The new protoype of the Omniclimber.

Table 5
OmniClimber VII characteristics.

Diameter × height Mass	260 × 140 mm 1120 g
Total number of actuators	7
Total number of DOFs	5
Mobile robot Actuation	3 Dynamixel MX-64 rotary actuators
Arm Actuation	2 Pololu gear motors
Switchable magnets actuation	2 Pololu gear motors
Mechatronics and control	ad-hoc home made control unit with ARM cortex microcontroller
Power	Thetered
Wheels	3 Omnidirectional Magnetic Wheels 70 mm diam.
Adhesion force∗	32 N (chassis switchable magnet *off*) 88 N (chassis switchable magnet *on*) 2 × 56 N (arm adhesion unit)
Max climbing speed	14 cm/s
90° plane transition time	15 s
Movement	omnidirectional

equipped with magnetic Rotary encoders that communicate with micro-controller trough SPI.

The communication between the board and a ground computer is achieved through a Bluetooth module which is integrated into the board. The ground computer communicates with the micro-controller trough UART and is used to establish communication with a computer where the User interface is running. Furthermore the board integrates a connection point to a Raspberry PI. This means that a Raspberry PI single board computer can be directly plugged into the board. Currently we use the Raspberry PI only for communication of videos to the ground computer through wi-fi. In the next versions we will use this single board computer for achieving some part of the high level control on the robot rather than on the ground computer. The actuators of the climbing mechanism are 3 Dynamixel MX-64 gear motors. While the communication is done wirelessly, the power supply is tethered.

7. Tests and results

Fig. 19 shows the new prototype of the Omniclimber. The OmniClimber was tested on structures made of 1 mm thick steel sheets. Fig. 20 shows the robot moving on the ground and approaching a steel locker, attachment of the SM unit, transitioning to the vertical plane and then climbing the structure. Fig. 21 shows a transition from a vertical plane to the ceiling.

Compared to the previous version of the Omniclimber [19] which benefited from a minimalistic approach in terms of actuation (i.e. only 4 actuators for the whole robot), this version is more complex and integrates seven actuators. Furthermore the mechanism has a better control over the arm resulting in a smooth transition action. Moreover, in addition to the adhesion force of the arm's adhesion unit, the adhesion force of the chassis to the structure can be controlled with switchable magnets. The non back drivable actuation system for the SM units result in a lower power consumption compared to electromagnets since the power is consumed only in the act of switching. This is also safer than electromagnets in case of a power failure. One drawback of the novel Omniclimber is its relatively slow transition which takes 15 seconds for a 90° plane transition.

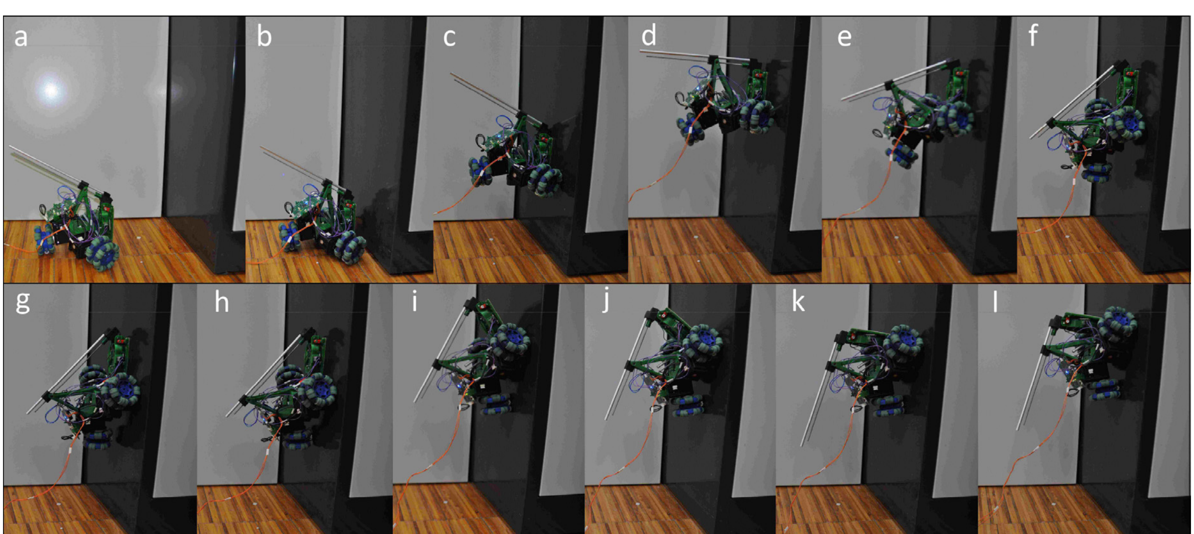

Fig. 20. Video frames of the robot performing the transition between the floor and a vertical surface.

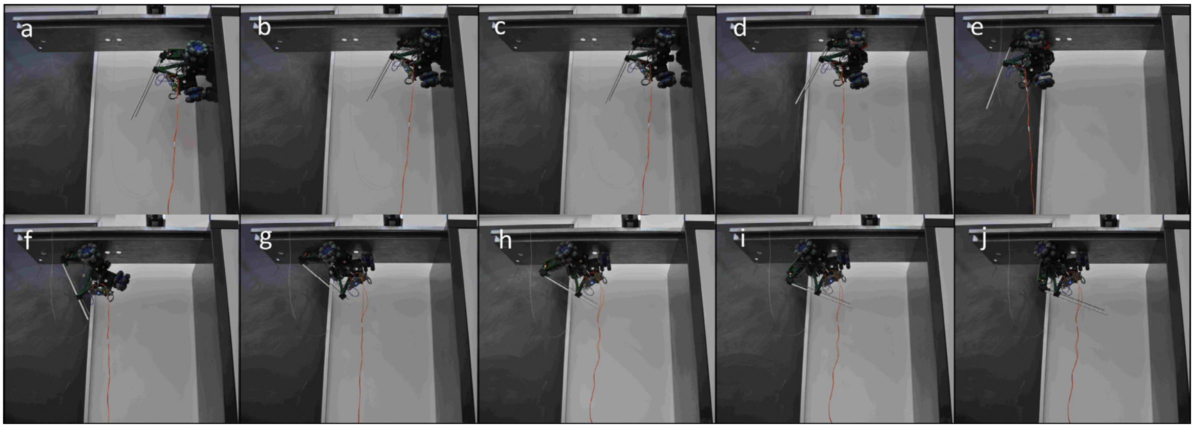

Fig. 21. Video frames of the robot performing the transition between a vertical wall and a celling.

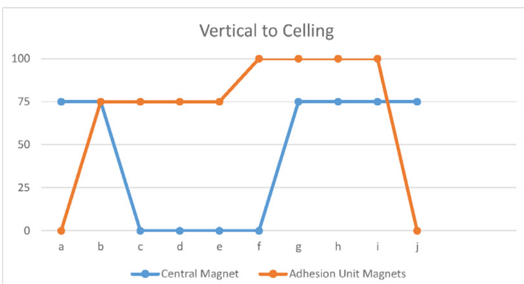

Fig. 22. Wall to ceiling maneuver results.

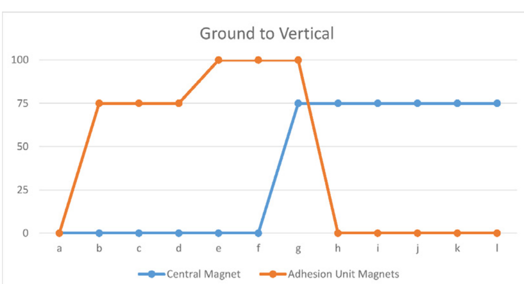

Fig. 23. Floor to wall maneuver results.

During a plane transition, the adhesion force of the switchable magnets of the chassis and the adhesion unit is controlled, in order to make the transition possible. At this stage we are not doing fine force control over the SMs. But we control the force at predefined intervals of 0, 25, 50 , 75 and 100 percent of the maximum force. Figs. 22 and 23, represent the percentage of the applied force to the maximum force of the SM units during the transitions, ground to a vertical wall and wall to the celling. The letters on the bottom axis represent the frames shown in Fig. 20. When climbing a vertical structure of 1mm thickness, the magnets of the wheel apply a vertical adhesion force of 9N. The magnets on the wheels are embedded to increase the wheels traction and reduce the slippage. The central magnet provides the main adhesion force for the robot chassis.

The characteristics of the OmniClimber version VII are presented in Table 5.

8. Conclusions

In this article we proposed a novel plane transition mechanism for the Omniclimbers based on switchable magnet units that can be controlled for precise adhesion force control. We simulated,designed and fabricated a custom design of the SM units for the specific applications considering to reduce the detachment torque and also maximize the force per mass ratio for thinner structures. SM units were installed on the arm and on the chassis of the robot. The SM on the chassis replaced the previous permanent magnet of the chassis. In this case we can opt the adhesion force based on the climbing structure.

The transition arm is composed of high ratio transmission mechanisms i.e., a 100:1 lead screw nut mechanism. The inverse kinematics of the transition mechanism were also presented. Furthermore, we designed, developed and integrated a home-made compact control unit that integrates the drivers and performs the closed loop control for all actuators and communicates with a PC through bluetooth.

The adhesion unit can be positioned accurately on the structure and is capable of raising the entire robot smoothly. The use of the switchable magnets allows for control over adhesion force which in necessary during transition and climbing. The precise control of the force generated by the magnets proved to be important for navigation and to switch between planes. Furthermore, adjustment of the adhesion force during the climbing is made easier.

The use of linear guides with threaded shafts is an effective way to achieve accurate movements with high force with small actuators and also to have a non back drivable system. In this way the arm can stay at any position without power consumption. However this comes at the cost of a slow transitions. Yet this is not critical, since the transition does not happen very often.

The novel SM based adhesion unit and also the novel transition arm showed several advantageous over the previous version. This new design allows better control of the transitions of the robot, by controlling its movement with two actuators instead of one, without increasing the robot's weight. The new version is 30% lighter and enables a smooth motion.

The reduced power consumption obtained by the use of switchable magnets, when comparing to electromagnets, potentially increases the autonomy and range of the OmniClimber climbing robot. Another advantage of using switchable magnets is that it makes the robot safer in the event of power failure, and enables adhesion force control, giving better adaptability to different surfaces. Experiments showed that the mechanism works as predicted and it is a viable solution for wheeled climbing robots. Current transition time is 15 seconds.

Future works will mainly focus on integration of proximity sensors on the arm and on the chassis and algorithms to make the transition autonomous.

The main limitation which is the subject of the future work is to be able to adjust the required force for the SM unit of the chassis based on the material and surface condition. In this way we can autonomously control this force. This will be achieved by measuring the wheels slippage by comparing the velocity of the wheels (measured by encoders) and the robot (measured by an optical flow sensor).

Acknowledgment

This research work was partially supported by the Portuguese Foundation of Science and Technology, contract SFRH/BPD/70557/2010, PTDC/EME-CRO/121547/2010 and SFRH/BD/94272/2013.

References

[1] Birkmeyer P, Gillies AG, Fearing RS. Clash: climbing vertical loose cloth. In: Intelligent robots and systems (IROS), 2011 IEEE/RSJ international conference on. IEEE; 2011. p. 5087–93.
[2] Unver O, Uneri A, Aydemir A, Sitti M. Geckobot: a gecko inspired climbing robot using elastomer adhesives. In: Robotics and automation, 2006. ICRA 2006. Proceedings 2006 IEEE international conference on. IEEE; 2006. p. 2329–35.
[3] Tsukagoshi H, Chiba H, Kitagawa A. Gel-type sticky mobile inspector to traverse on the rugged wall and ceiling. In: Robotics and automation, 2009. ICRA'09. IEEE international conference on. IEEE; 2009. p. 1591–2.
[4] Balaguer C, Pastor J, Giménez A, Padrón V, Abderrahim M. Roma: a multifunctional autonomous self-supported climbing robot for inspection application. In: 3rd IFAC symposium on intelligent autonomous vehicles. Madrid, Spain; 1998. p. 357–62.
[5] Balaguer C, Gimenez A, Pastor J, Padrón V, Abderrahim M. A climbing autonomous robot for inspection applications in 3d complex environments. Robotica 2000;18:287–97.
[6] Tavakoli M, Marjovi A, Marques L, de Almeida A. 3DCLIMBER: a climbing robot for inspection of 3d human made structures. In: IEEE/RSJ international conference on intelligent robots and systems, IROS. Nice–Paris; 2008. p. 4130–5.
[7] Aracil R, Saltarén R, Sabater J. TREPA, parallel climbing robot for maintenance of Palm trees and large structures. Proc 2nd international workshop & conference on climbing & walking robots (CLAWAR) 1999:453–61.
[8] Tavakoli M, Zakerzadeh M, Vossoughi G, Bagheri S. Design and prototyping of a hybrid pole climbing and manipulating robot with minimum DOFs for construction and service Applications. In: Climbing and walking robots: proceedings of the 7th international conference clawar 2004; 2005.
[9] Balaguer C, Gimenez A, Abderrahim C. ROMA robots for inspection of steel based infrastructures. Ind Robot: An Int J 2002;29(3):246–51.
[10] Hussain S, Sattar T, Salinas E. Parameter analysis and design framework for magnetic adhesion wall climbing wheeled robot. Int J Intell Syst Technol Appl 2012;11(1):102–16.
[11] Silva M, Barbosa R, Oliveira A. Computational Intelligence and Decision Making. Intelligent Systems, Control and Automation: Science and Engineering, 61. Springer; 2013. p. 301–11.
[12] Eich M, Vogele T. Design and control of a lightweight magnetic climbing robot for vessel inspection. In: Control & automation (MED), 2011 19th mediterranean conference on. IEEE; 2011. p. 1200–5.
[13] Rochat F, Schoeneich P, Lüthi B, Bleuler H, Moser R, Mondada F. CY-MAG3D: a simple and miniature climbing robot with advance mobility in ferromagnetic environment. Ind Robot: An Int J 2011;38(3):229–33.
[14] Tâche F, Fischer W, Caprari G, Siegwart R, Moser R, Mondada F. Magnebike: a magnetic wheeled robot with high mobility for inspecting complex-shaped structures. J Field Robotics 2009;26(5):453–76.
[15] Fischer W, Tâche F, Siegwart R. Magnetic wall climbing robot for thin surfaces with specific obstacles. In: Field and service robotics. Berlin Heidelberg: Springer; 2008. p. 551–61.
[16] Lauria M, Piguet Y, Siegwart R. Octopus-an autonomous wheeled climbing robot. In: Proceedings of the fifth international conference on climbing and walking robots, vol. 322. Citeseer; 2002.
[17] Lee W, Hirai M, Hirose S. Gunryu III: reconfigurable magnetic wall-climbing robot for decommissioning of nuclear reactor. Adv Robotics 2013;27(14):1099–111.
[18] Longo D, Muscato G. A modular approach for the design of the alicia climbing robot for industrial inspection. Ind Robot: An Int J 2004;31(2):148–58.
[19] Viegas C, Tavakoli M. A single DOF arm for transition of climbing robots between perpendicular planes. In: Intelligent robots and systems (IROS 2014), 2014 IEEE/RSJ international conference on. IEEE; 2014. p. 2867–72.
[20] Gilpin K, Kotay K, Rus D, Vasilescu I. Miche: modular shape formation by self--disassembly. Int J Robotics Res 2008;27(3-4):345–72.
[21] Rochat F, Beira R, Bleuler H, Mondada F. Tremo: an inspection climbing inchworm based on magnetic switchable device. In: Field robotics: Proceedings of the 14th international conference on climbing and walking robots and the support technologies for mobile machines. EPFL-CONF-165651. World Scientific; 2011. p. 421–8.
[22] Rochat F, Schoeneich P, Bonani M, Magnenat S, Mondada F, Bleuler H, et al. Design of magnetic switchable device (MSD) and applications in climbing robot. In: Emerging trends in mobile robotics. EPFL-CONF-151772. World Scientific; 2010. p. 375–82.
[23] Tavakoli M, Marques L, de Almeida A. Omniclimber: an omnidirectional light weight climbing robot with flexibility to adapt to non-flat surfaces. In: Intelligent robots and systems (IROS), 2012 IEEE/RSJ international conference on; 2012. p. 280–5. doi:10.1109/IROS.2012.6385454.
[24] Tavakoli M, Viegas C, Marques L, Pires JN, de Almeida AT. Magnetic omnidirectional wheels for climbing robots. In: Intelligent robots and systems (IROS), 2013 IEEE/RSJ international conference on. IEEE; 2013. p. 266–71.
[25] Tavakoli M, Viegas C. Analysis and application of dual-row omnidirectional wheels for climbing robots. Mechatronics 2014;24(5):436–48. http://dx.doi.org/10.1016/j.mechatronics.2014.04.003.
[26] Tavakoli M, Lopes P, Sgrigna L, Viegas C. Motion control of an omnidirectional climbing robot based on dead reckoning method. Mechatronics 2015;30:94–106.
[27] COMSOL. Software multiphisics. [Online] Available: https://wwwcomsolpt/2015.
[28] HKCM. Magnet distributor. [Online] Available: https://wwwhkcmde/expertphp?fav=2005.